Optimal Configurations of ACLD/Plate for Bending Vibration Control using INSGA-II

Dongdong Zhang[1]; Ling Zheng[2]; Yinong Li[3]

Chongqing University, China

ABSTRACT

Active constrained layer damping (ACLD) has been demonstrated as an effective means of vibration and noise control for flexible structure. The overall performance of ACLD system is governed by the performance of the passive and the active controls on which the configurations of ACLD treatments have significant effect. In this paper, a multi-objective optimization model for ACLD treatments is established based on the finite element model of the plate partially covered with ACLD treatments. The improved non-dominated sorting genetic algorithm (INSGA-II) is developed to obtain the optimal configurations of ACLD treatments for vibration control of bending modes of the plate. In the optimization procedure, an integrated multi-objective optimization strategy is proposed, in which the passive and the active controls performance are considered simultaneously. The modal loss factors and the frequency response excited by the unit control voltage are selected as the passive and active control objectives, respectively. The location-numbering of the ACLD patches and the thickness of the viscoelastic materials (VEM) and piezoelectric material (PEM) are served as design variables. The vibration control results show that the better results of vibration control can be achieved in passive and active control when the optimal ACLD treatments are employed.

Keywords: Active constrained layer damping, finite element model, INSGA-II, integrated multi-objeceive optimization, I-INCE Classification of Subjects Number(s): 46.4

1. INTRODUCTION

Vibration and noise control of flexible structure is a common subject of engineering community. Active Constrained Layer Damping (ACLD) treatment has been used widely for damping the vibration of beams [1-2], plates [3] and shells[4]. The ACLD treatment generally consists of a viscoelastic layer, which dissipates the vibration energy through shear deformation, and a piezoelectric constrained layer, acting as active actuators when proper active control means is applied to enhance the dissipation energy characteristics.

The overall performance of the ACLD system is governed by performance of the passive control and the active control [5]. And in practice, to obtain the optimal performance, the ACLD treatment is usually cut into several segments. Thus, the optimization for the ACLD system consists of two parts, one is optimum design of the passive control of ACLD system, e.i PCLD system, and the other is the active control system.

Optimization for PCLD system is essential to maximize the performance of the ACLD system. Furthermore, with optimally designed PCLD treatment, the performance is guaranteed to be robust even if the active component of the ACLD ceases to operate or fail [5]. Kung and Singh [6] developed an energy-based approach of multiple constrained layer damping patches. The optimal configurations of constrained layer damping patches for several separate vibration modes were investigated. Baz[5] optimized the placement of ACLD patches using the modal strain energy(MSE) method. In this study, the total weight of the damping treatments is taken as the objective function while satisfying constrained imposed on the modal damping ratios. Zheng and Cai[7]employed different nonlinear optimization methods/algorithms, such as sub-problem approximation method, the first-order method,

[1] cquzhdd@gmail.com
[2] zling@cqu.edu.cn
[3] beifang.dehe@163.com

sequential quadratic programming(SQP) and genetic algorithm (GA), to obtain the optimal locations and lengths of the PCLD patches with aim to minimize displacement amplitude of the middle beam. Al-Ajmi and Bourisli [8] optimized the PCLD segments' length for a single mode using genetic algorithm (GA). Zheng Ling [9-10] considered the PCLD structure optimization as a topology optimization problem, and an optimality criterion and evolutionary structural optimization (ESO) method were employed to find the optimal configuration of the PCLD treatments. In many of these studies, the locations of the PCLD patches, the thickness of the CLD and VEM were optimized, but there was a limitation that the effect of all the parameters was seldom taken into account at the same time. Additionally, only a single objective function was took into account to find the optimal configurations of PCLD treatments.

The closed-loop performance of ACLD system is determined by the parameters of active constrained layer (acting as piezo-electric actuators) and controller. In open literatures, many works [11-15] can be found where different optimization methods were applied in pure active vibration controls, but only a few were related to closed-loop optimization of ACLD system. Hau[16] presented a multi-objective genetic algorithm (MOGA) to solve an integrated optimization problem for the ACLD beams. The thickness of the CLD and VEM, the locations of the ACLD patches and the control gains were optimized simultaneously. Araújo[17]addressed a new form of ACLD system, where piezoelectric patch sensors and actuators are bonded to the exterior faces of a sandwich plate. And the optimal placement of the co-located pairs of piezoelectric patch actuators was obtained using Direct Multi-Search (DMS) method. The aforementioned research efforts show that the performance of ACLD system/pure active vibration control is improved when the sensors/actuators placement and the parameters of controller are optimized. However, for all almost of the efforts in the literature, the optimal placement of sensors/actuators are coupled with parameters of the different controllers.

In the present work, the objective is to develop an integrated optimization strategy that enables to obtain optimal performance of passive control and active control system for ACLD system simultaneously. And it is noteworthy that only the configurations of actuators is optimized, making the active control performance of ACLD system uncoupled with the parameters of controller.

This paper is organized in five sections. In section 1, the brief introduction is given. In section 2, the multi-objective optimization problem for ACLD system is formulated based on finite element method (FEM) and an integrated optimization strategy is proposed. In section 3, the optimization algorithm is described and improved. In section 4, the multi-objective optimization procedures for ACLD system are carried out and effectiveness of the optimization strategy is verified. The vibration control results of the ACLD system are analyzed for different multi-objective optimization configurations. Finally, concluding remarks are given in section 5.

2. PROBLEM FORMULATION

2.1 Finite Element Model

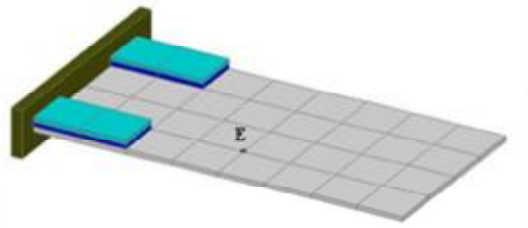

Figure 1 –The cantilever plate treated with ACLD patches

A finite element model is presented to analyze the dynamic characteristic of plates treated with active constrained layer damping (ACLD). Figure 1 illustrates a cantilever plate partially treated with ACLD patches. The viscoelastic material (VEM) layer is bonded to the base plate, and the top layer is served as the active constrained layer to enhance the shear deformation consuming the vibration energy of the base structure.

2.1.1 Shape functions

A two-dimensional element with four nodes referred in [18] is used to discrete the ACLD/plate system in the finite element model. Each node has seven degrees of freedom, including the longitudinal displacements u_c and v_c of the constrained layer, the longitudinal displacements u_b , v_b of the base plate, the lateral displacement w of the whole structure, and the slopes q_x , q_y of lateral

displacement. The displacement at any point in the element can be described as follows

$$\{u_c \quad v_c \quad u_b \quad v_b \quad w \quad w_{,x} \quad w_{,y}\}^T = \{\mathbf{S}_{uc} \quad \mathbf{S}_{vc} \quad \mathbf{S}_{ub} \quad \mathbf{S}_{vb} \quad \mathbf{S}_w \quad \mathbf{S}_{w,x} \quad \mathbf{S}_{w,y}\}^T \mathbf{q}^e \tag{1}$$

Considering the relationship of kinematics formations among the layers of the ACLD/plate, the shape functions for the longitudinal displacements u_v, v_v and the shear deformations g_x, g_y of the VEM core can be derived as[4]

$$\mathbf{S}_{uv} = \frac{1}{2}\left[(\mathbf{S}_{uc} + \mathbf{S}_{ub}) - \frac{h_c - h_b}{2}\mathbf{S}_{w,y}\right], \quad \mathbf{S}_{vv} = \frac{1}{2}\left[(\mathbf{S}_{uc} + \mathbf{S}_{ub}) + \frac{h_c - h_b}{2}\mathbf{S}_{w,x}\right]$$

$$\mathbf{S}_{gx} = \frac{1}{h_v}\left[(\mathbf{S}_{uc} - S_{ub}) - \left(\frac{h_c + h_b}{2} + h_v\right)\mathbf{S}_{w,y}\right], \mathbf{S}_{gy} = \frac{1}{h_v}\left[(\mathbf{S}_{uc} - \mathbf{S}_{ub}) + \left(\frac{h_c + h_b}{2} + h_v\right)\mathbf{S}_{wx}\right] \tag{2}$$

So the displacement vector of the VEM can be expressed as

$$\{u_v \quad v_v\} = \{\mathbf{S}_{uv} \quad \mathbf{S}_{vv}\}\mathbf{q}^e \tag{3}$$

$$\{g_x \quad g_y\} = \{\mathbf{S}_{gx} \quad \mathbf{S}_{gy}\}\mathbf{q}^e \tag{4}$$

2.1.2 Potential energies

The potential energies related with the plane stress deformations of the ACLD/plate system can be expressed as

$$P_{pi} = \frac{E_i h_i}{2(1-m_i^2)}\int_{-a}^{a}\int_{-b}^{b}\left[\left(\frac{\partial u_i}{\partial x}\right)^2 + \left(\frac{\partial v_i}{\partial y}\right)^2 + 2m_i\frac{\partial u_i}{\partial x}\frac{\partial v_i}{\partial y} + \left(\frac{1-m_i}{2}\right)\left(\frac{\partial u_i}{\partial y} + \frac{\partial v_i}{\partial x}\right)^2\right]dxdy \tag{5}$$

where $i = b, c, v$ denote the base plate, the active constrained layer and the viscoelastic layer, respectively. E_i, m_i are Young's modulus and Passion's ratio, and h_i is the thickness for the three layer in the ACLD/plate system, respectively. Substituting equation (1) into equation (5) for base plate and active constrained layer, the P_{pi} can be obtained as follows

$$P_{pi} = \frac{1}{2}(\mathbf{q}^e)^T h_i \int_{-a}^{a}\int_{-b}^{b}\mathbf{B}_{pi}^T\mathbf{D}_i\mathbf{B}_{pi}dxdy(\mathbf{q}^e) \quad i = b, c \tag{6}$$

where $\mathbf{D}_i$ is the elastic coefficient matrix and $\mathbf{B}_{pi} = \left[\frac{\partial \mathbf{S}_{ui}}{\partial x} \quad \frac{\partial \mathbf{S}_{vi}}{\partial y} \quad \frac{\partial \mathbf{S}_{ui}}{\partial y} + \frac{\partial \mathbf{S}_{vi}}{\partial x}\right]^T$. So the membrane stiffness matrices for the base plate and the constrained layer can be defined as

$$\mathbf{k}_{pi} = h_i \int_{-a}^{a}\int_{-b}^{b}\mathbf{B}_{pi}^T\mathbf{D}_i\mathbf{B}_{pi}dxdy \quad i = b, c \tag{7}$$

Substituting equation (3) into equation (5) for viscoelastic layer, the P_{pv} from which the h_b, h_c, h_v are factored out is expressed as follows

$$P_{pv} = \frac{1}{2}(\mathbf{q}^e)^T(\mathbf{k}_{1v} + \mathbf{k}_{2v} + \mathbf{k}_{3v} + \mathbf{k}_{4v})(\mathbf{q}^e) \tag{8}$$

So the membrane stiffness matrices for viscoelastic layer can be defined as

$$\mathbf{k}_{pv} = \mathbf{k}_{1v} + \mathbf{k}_{2v} + \mathbf{k}_{3v} + \mathbf{k}_{4v} \tag{9}$$

Meanwhile, the potential energies related with the bending deformations of the ACLD/plate system are expressed as

$$P_{bi} = \frac{E_i h_i^3}{24(1-m_i^2)}\int_{-a}^{a}\int_{-b}^{b}\left[\left(\frac{\partial^2 w}{\partial x^2}\right)^2 + \left(\frac{\partial^2 w}{\partial y^2}\right)^2 + 2m_i\frac{\partial^2 w}{\partial x^2}\frac{\partial^2 w}{\partial y^2} + 4\left(\frac{1-m_i}{2}\right)\left(\frac{\partial^2 w}{\partial x \partial y}\right)^2\right]dxdy, i = b, c, v \tag{10}$$

Substituting equation (1) into equation (10), the P_{bi} can be obtained as follows

$$P_{bi} == \frac{1}{2}(\mathbf{q}^e)^T \frac{h_i^3}{12}\int_{-a}^{a}\int_{-b}^{b}(\mathbf{B}_{bi})^T\mathbf{D}_i\mathbf{B}_{bi}dxdy(\mathbf{q}^e) \quad i = b, c, v \tag{11}$$

where $\mathbf{B}_{bi} = \left[\frac{\partial^2 \mathbf{S}_w}{\partial x^2} \quad \frac{\partial^2 \mathbf{S}_w}{\partial y^2} \quad 2\frac{\partial^2 \mathbf{S}_w}{\partial x \partial y}\right]^T$. So the bending stiffness matrices for every layer in the ACLD/plate system can be defined as

$$\mathbf{k}_{bi} = \frac{h_i^3}{12}\int_{-a}^{a}\int_{-b}^{b}\mathbf{B}_{bi}^T\mathbf{D}_i\mathbf{B}_{bi}\,dxdy \quad i=b,c,v \tag{12}$$

For the ACLD/plate system, the vibration energy is consumed by the shear deformation of the VEM. The potential energy related with the shear deformations of the VEM is derived as:

$$P_{sv} = \frac{1}{2}\int_V \left(g_x G g_x + g_y G g_y\right)dV \tag{13}$$

where G_v is the shear modulus of the VEM. Substituting equation (4) into equation (13), the P_{sv}, like the potential energy P_{pv}, can be obtained as follows

$$P_{v3} = \frac{1}{2}\left(\mathbf{q}^e\right)^T\left(\mathbf{k}_{1sv} + \mathbf{k}_{2sv} + \mathbf{k}_{3sv}\right)\left(\mathbf{q}^e\right) \tag{14}$$

So the shear stiffness matrices for viscoelastic layer is obtained as

$$\mathbf{k}_{sv} = \mathbf{k}_{1sv} + \mathbf{k}_{2sv} + \mathbf{k}_{3sv} \tag{15}$$

2.1.3 Kinetic energies

The kinetic energy for each layer of the ACLD/plate system are expressed as

$$T_i = \frac{1}{2}r_i h_i\int_{-a}^{a}\int_{-b}^{b}\left[\left(\frac{\partial u_i}{\partial t}\right)^2 + \left(\frac{\partial v_i}{\partial t}\right)^2 + \left(\frac{\partial w}{\partial t}\right)^2\right]dxdy \tag{16}$$

where $i=b,c,v$ denote the base plate, the constrained layer and the viscoelastic layer, respectively. r_i, h_i are density and the thickness for the three layers in the ACLD/plate system, respectively. Substituting equation (1) into equation (16) for base plate and constrained layer, the T_i can be obtained as follows

$$T_i = \frac{1}{2}\left(\dot{\mathbf{q}}^e\right)^T r_i h_i\int_{-a}^{a}\int_{-b}^{b}\left[\left(\mathbf{S}_{ui}\right)^T\mathbf{S}_{ui} + \left(\mathbf{S}_{vi}\right)^T\mathbf{S}_{vi} + \left(\mathbf{S}_w\right)^T\mathbf{S}_w\right]dxdy\left(\dot{\mathbf{q}}^e\right) \tag{17}$$

So the element mass matrices for the base plate and the constrained layer can be defined as

$$\mathbf{m}_i = r_i h_i\int_{-a}^{a}\int_{-b}^{b}\left[\left(\mathbf{S}_{ui}\right)^T\mathbf{S}_{ui} + \left(\mathbf{S}_{vi}\right)^T\mathbf{S}_{vi} + \left(\mathbf{S}_w\right)^T\mathbf{S}_w\right]dxdy \tag{18}$$

For viscoelatic layer, like the stiffness matrix, the element mass matrix can be defined as

$$\mathbf{m}_v = \mathbf{m}_{1v} + \mathbf{m}_{2v} + \mathbf{m}_{3v} \tag{19}$$

2.1.4 Work done by the external force and control force [4]

The virtual work done by the external disturbance is

$$W_d = \left(\mathbf{q}^e\right)^T\mathbf{F}_d^e + \left(\mathbf{q}^e\right)^T\mathbf{F}_c^e \tag{20}$$

2.1.5 Dynamic equation of motion

Assembling the ACLD system for all elements yields the dynamic equation of the plate with ACLD treatments,

$$\mathbf{M}\ddot{\mathbf{q}} + \left(\mathbf{K} + G_v\mathbf{K}_{sv}\right)\mathbf{q} = \mathbf{F}_d + \mathbf{F}_c \tag{21}$$

Here, to describe the frequency-dependent behavior of the visco-elastic material, the shear modulus of VEM is modeled using Golla-Hughes-McTavish (GHM) method [19]. So The global equations of motion can be rewritten as follows

$$\mathbf{M}\ddot{\mathbf{X}} + \mathbf{C}\dot{\mathbf{X}} + \mathbf{K}\mathbf{X} = \mathbf{F}_d + \mathbf{F}_c \tag{22}$$

2.2 Multi-objective Optimal Design Formulation

A constrained multi-objective optimization problem for ACLD/plate can be mathematically written as

$$\begin{aligned} &\max \quad f_i(d) \qquad i = 2, \mathbf{L}\, m \\ &s.t \quad c_j(d) \le 0 \quad j = 1, \mathbf{L}\, n \end{aligned} \tag{23}$$

where d denotes the design variables.

2.2.1 Objective functions

The state space model of the ACLD/plate can be obtained based on equation (22), as follows,

$$\begin{aligned} \dot{\mathbf{x}}(t) &= \mathbf{A}\mathbf{x}(t) + \mathbf{B}_d\mathbf{f}_d + \mathbf{B}_c\mathbf{f}_c \\ \mathbf{y}(t) &= \mathbf{C}\mathbf{x}(t) \end{aligned} \tag{24}$$

where the state space vector $\mathbf{x}(t)$ is chosen as $\{\mathbf{X}(t) \quad \dot{\mathbf{X}}(t)\}^T$, $\mathbf{A}$ is system matrix, $\mathbf{B}_d$ and $\mathbf{B}_c$ are the disturbance input matrices and the control force distribution matrices. $\mathbf{C}$ is the output matrix and $\mathbf{y}(t)$ is the output vector.

Based on the state space model of ACLD/plate, the complex eigenvalues of system matrix A can be expressed as

$$l_i(A) = a_i \pm jw_i^2 \tag{25}$$

where a_i and w_i^2 are the real and imaginary parts of the *i*th complex eigenvalues, respectively, and $j = \sqrt{-1}$. Here, the loss factor, which is related to performance of passive control for ACLD/plate, is defined as the passive objective function,

$$h_i(A) = -\frac{a_i}{w_i^2} \tag{26}$$

Obviously, the loss factor is larger, the vibration of the structure is more effectively suppressed when the ACLD treatments is in passive control mode.

The response value at measurement point when unit sinusoidal control voltage is applied on ACLD patches, is designed as active control objective,

$$z_i(P) = 20\lg(x) \tag{27}$$

where x denotes response value at measurement point P. Based on the active vibration control principle, larger $z_i(P)$ implies that the corresponding ACLD patches configuration can suppress the vibration of some measurement point more effectively.

Hence, the objective functions for multi-objective optimization of ACLD/plate are set to be

$$f(d) = \{h_i(A) \quad z_i(P)\} \tag{28}$$

2.2.2 Hybrid Design variables

The thickness of viscoelastic material (VEM) and piezoelectric constrained layer material (PCLM) the locations of the ALCD patches on the base plate are employed as the design variables. i.e.

$$d = \{l_i \quad h_{vj} \quad h_{ck}\} \qquad i = 1, \mathbf{L}\, s,\ l_i \neq l_p \ for\ i \neq p;\ \ j = 1, \mathbf{L}\, n;\ \ k = 1, \mathbf{L}\, m \tag{29}$$

where l_i is expressed by the positive integer, denoting the location-numbering of the ith ACLD patches, and h_{vj} and h_{ck} are expressed by positive continuous real number, denoting the thickness of VEM and PCLM. Thus, the design variable vector contains different variable type, i.e. a hybrid variable vector.

2.2.3 Constraints

Considering design requirements for practical engineering structures, the natural frequencies shift of base structure should be in a limited range, i.e.

$$\left| f_j - f_o \right| - c \leq 0 \tag{30}$$

where, f_o and f_j are the natural frequencies of the base structure and the ACLD/plate after optimization procedure is carried out.

3. OPTIMIZATION STRATEGY AND ALGORITHM

3.1 Optimization Strategy

An integrated optimization strategy is proposed with the aim of the performance of passive control and active control for ACLD/structure being optimized simultaneously. The highlight is that the optimal configurations of ACLD patches serving as actuators are achieved without consideration of active control algorithm. The strategy is described as follows, and the flow chart is shown in figure 2.

Step 1: the configurations of ACLD patches, including the thickness of active constrained layer and VEM, the location-numbering of the ACLD patches, are initialized.

Step 2: the passive control objective functions are calculated.

Step3: the optimal ACLD patches acting as actuators are searched from the initialized configurations, and the active control objective functions are calculated.

Step 4: evaluate the configurations of the ACLD patches.

Step 5: update the configurations of the ACLD patches, and step 2, 3 and 4 are carried out again until the optimal configurations of ACLD patches are obtained.

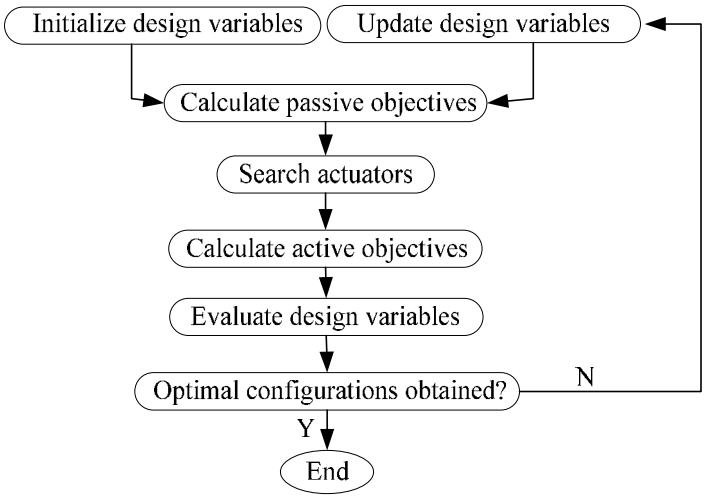

Figure 2 –The flow chart of integrated optimization for ACLD/structrue

3.2 Optimization Algorithm

For multi-objective optimization for ACLD/structure, the relationship between the design variables and the objectives is difficult to be described using explicit mathematical equations. Meanwhile, the design variables space composes of two different types of design variables: discrete and continuous. Hence, the traditional optimization strategies are difficult to solve this problem. In this paper, to overcome these problems, the non-dominated sorting genetic algorithm (NSGA-II), which combines with Direct Search method, is introduced and improved to solve the integrated multi-objective optimization problem.

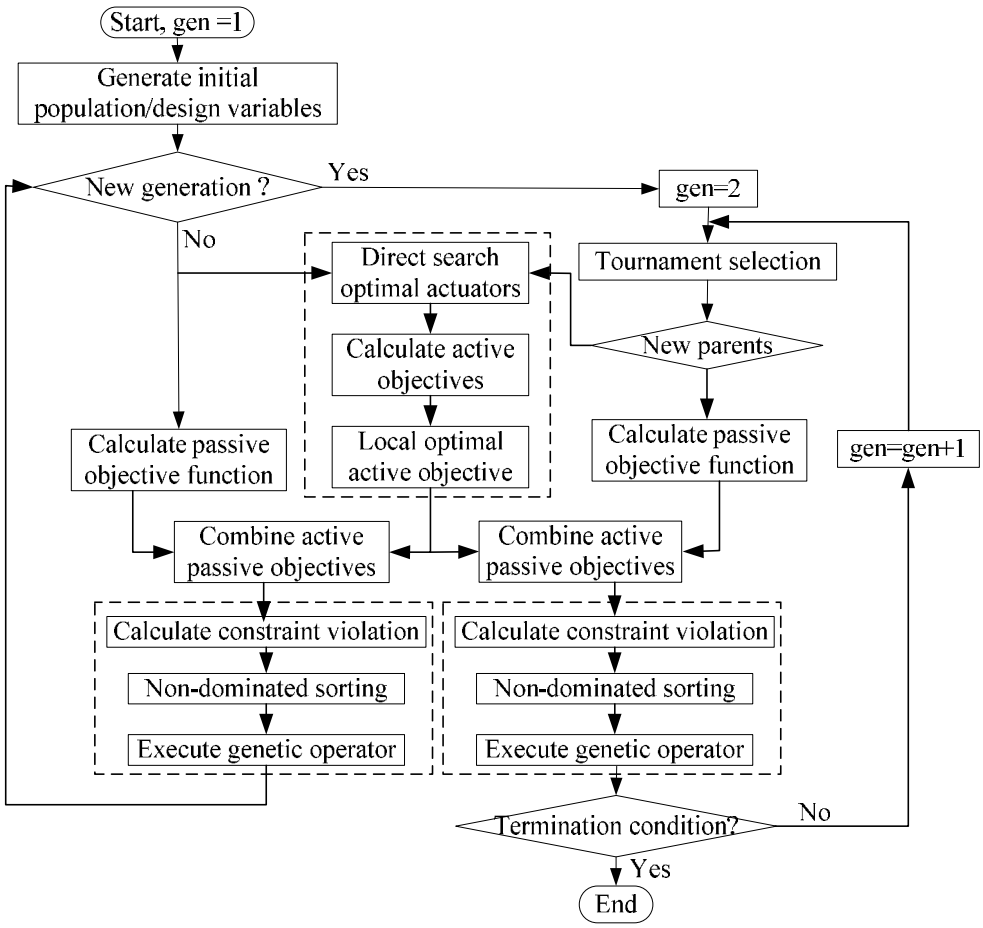

Figure 3 –Flow chart of the optimization algorithm.

The basic flow chart of the improved NSGA-II algorithm considering constraints is employed to

carry out the optimization shown in figure 3. Some basic ideals are explained as follows

(1) Chromosome representation. In this investigation, all the value of the design variables is encoded by decimal code. For simplicity, the chromosome constructions of hybrid variables, objective function value, constraint violation value, the rank value, the crowding distance, is shown in figure 4.

(2) Constraint handling. In the multi-optimization problem, the constraint violation is described as

$$g = \left| \frac{\left| f_j - f_o \right|}{c} - 1 \right| \tag{31}$$

In the constraint handling approaches, a tournament selection is employed where two solutions are compared at a time, and the following criteria are always enforced [20]

a) Any feasible solution is preferred to any infeasible solution.

b) Among two feasible solutions, the one having smaller constraint violation is preferred.

c) Among two infeasible solutions, the one having smaller constraint violation is preferred.

(3) Non-dominated sorting. The constrain-domination sorting for any two solutions is referred in[21].

(4) Crowding distance. The crowding distance of the ith solution (marked with solid circles) in its front which is shown in figure 5, is the average side-length of the cuboids (shown by a dashed box). It denotes the diversity distribution of the solution in its front.

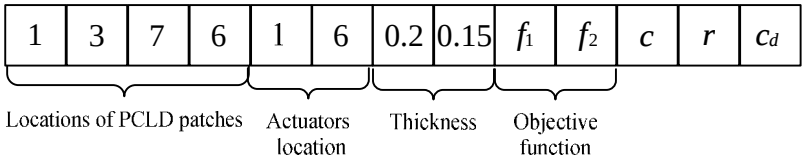

Figure 4 –Chromosome constructions. c denote the constraint violation value, r denotes the rank value for ith solution, c_d denotes the crowding distance of the ith solution

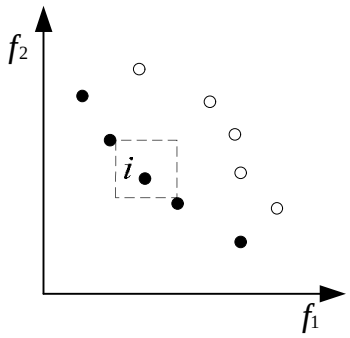

Figure 5 –The crowding distance calculation.

(5) The genetic operator

In this paper, the new genetic operators are introduced and improved for the special optimization problem of the ACLD/plate.

a) The new crossover operator

The Laplace crossover operator which is proposed in [22], is introduced in the NSGA-II to deal with the hybrid/mixed design variables optimization problems. According to the Laplace crossover operator, the two offspring produced by the two parents, x_i^1, x_i^2 are computed as

$$\begin{aligned} y_i^1 &= x_i^1 + a_i \left| x_i^1 - x_i^2 \right| \\ y_i^2 &= x_i^2 + a_i \left| x_i^1 - x_i^2 \right| \end{aligned} \tag{32}$$

where $a_i = \begin{cases} a - b\log(u_i) & r_i \le 1/2 \\ a - b\log(u_i) & r_i > 1/2 \end{cases}$, u_i, r_i are uniform random numbers between 0 and 1, $a \in R$ is called location parameter, and $b > 0$ is termed as scale parameter. For integer design variables, $b = b_{\text{int}}$, is usually assigned to be a integer, otherwise, $b = b_{real}$ is set to be a positive real value below 1. For smaller value of b, offspring are expected to be produced near the parents, and for lager b, offspring are likely to be produced far from parents.

Due to two or more ACLD patches can not be bonded on the same location on the base plate, i.e., $l_i \neq l_j$ for $i \neq j$, thus, the procedure of the original crossover operator will be modified. Based on the smallest distance principle, the crossover operator will be carried out for every pair variables denoting the locations of CLD patches in the parent. The procedure is expressed as follows,

Step 1: The crossover operator is carried out for the first pair variables l_1^{p1} and l_1^{p2} in the parent and the first two offspring are got as follows

$$\begin{matrix} \{l_1^{p1} & l_2^{p1} & l_3^{p1} & l_4^{p1}\} \\ \{l_1^{p2} & l_2^{p2} & l_3^{p2} & l_4^{p2}\} \end{matrix} \Rightarrow \begin{matrix} \{l_1^{c1} & 0 & 0 & 0\} \\ \{l_1^{c2} & 0 & 0 & 0\} \end{matrix} \tag{33}$$

Step 2: The range $S_{l_2^{c1}}$ and $S_{l_2^{c2}}$ for the second two offspring are updated to

$$S_{l_2^{c1}} = S_l - l_1^{c1}, S_{l_2^{c2}} = S_l - l_1^{c2} \tag{34}$$

Step 3: The crossover operator is carried out for the first pair variables l_2^{p1} and l_2^{p2} in the parent and the second two offspring are obtained as follows

$$\begin{matrix} \{l_1^{p1} & l_2^{p1} & l_3^{p1} & l_4^{p1}\} \\ \{l_1^{p2} & l_2^{p2} & l_3^{p2} & l_4^{p2}\} \end{matrix} \Rightarrow \begin{matrix} \{l_1^{c1} & l_2^{c1} & 0 & 0\} \\ \{l_1^{c2} & l_2^{c2} & 0 & 0\} \end{matrix} \tag{35}$$

If $l_1^{c1} \equiv l_2^{c1}$ or $l_1^{c2} \equiv l_2^{c2}$, then l_2^{c1} and l_2^{c2} will be revised as

$$l_2^{c1} = \min\left(\left|S_{l_2^{c1}} - l_2^{c1}\right|\right) l_2^{c2} = \min\left(\left|S_{l_2^{c2}} - l_2^{c2}\right|\right) \tag{36}$$

Step 4: Step 2 and Step 3 are continued until the crossover operator is carried out for every integer variable pair.

b) The new mutation operator

The power operator which is proposed in [21], is introduced in the NSGA-II as mutation operator to deal with the hybrid/mixed design variables optimization problems. According to the mutaion operator, the offspring produced by the parents, x_i^m, is generated as:

$$y_i^m = \begin{cases} x_i^m - s(x_i^m - x_i^l) & t < r \\ x_i^m + s(x_i^u - x_i^m) & t \geq r \end{cases} \tag{37}$$

where $s = (s_1)^p$, s_1 is an uniform random number in the range of 0 to 1, p is named as the power distribution index of mutation. $p = p_{\text{int}}$, is usually assigned to be a positive integer for integer design variables, otherwise, $p = p_{real}$ is set to be a positive real value less than 1. For large values of p , more diversity in the solutions is expected, and for small valves of p , less perturbance is achieved. $t = (x_i^m - x_i^l)/(x_i^u - x_i^m)$, x_i^l, x_i^u are lower and upper limits of the ith design variable. r is a uniformly distributed random number between 0 and 1.

When the mutation operator is carried out for integer variables, the similar procedure like that of the crossover operator is employed.

After the crossover and mutation operator are performed, the variables denoting the locations of CLD patches are truncated to integer.

4. OPTIMIZATION RESULTS AND DISCUSSION

4.1 The cantilever ACLD/plate

A cantilever ACLD/plate is modeled based on the above formulation. It is divided into 8×4 elements shown in figure 6.The left side of the plate is clamped. The numbers on the element denote the locations for ACLD patches which will be bonded on the base plate, as well as the element numbering. The base plate, with the size of 0.2×0.1m2, is partly treated with ACLD treatments. The main physical parameters of the base plate (Aluminum), viscoelastic layer (ZN-1) and active piezoelectric layer (P-5H) are listed in table 1.

The multi-objective optimization problem for ACLD/plate is established. The first mode loss factor is selected as passive objective functions, and response value at measurement point induced by unit sinusoidal control voltage (frequency equal to the first mode frequency) are taken as active control

objective. The number of PCLD patches is selected as eight, and two of the eight patches are selected as actuators. In the following optimization procedure, the range of thickness is that $0.0001m \le h \le 0.002m$.

Table1– Geometrical and Physical Parameters of ACLD/plate system

Aluminum		P-5H		ZN-1			
h_b	0.0008m	h_c	0.0005m	h_v	0.001m	V_1	148.0
E_b	69GPa	E_c	74.5GPa	m_v	0.3	V_2	12.16
m_b	0.3	m_c	0.32	r_v	789.5 kg/m^3	V_3	810.4
r_b	2800kg/m^3	r_c	7450kg/m^3	G^∞	554200Pa	w_1	896200
		d_{31} , d_{32}	186×10^{-12}C/N	a_1	3.960	w_2	927800
				a_2	65.69	w_3	761300

4	8	12	16	20	24	28	32
3	7	11	15	19	23	27	31
2	6	10	14	18	22	26	30
1	5	9	13	17	21	25	29

Figure 6 –Finite element partition of the ACLD/plate

4.2 Results and discussion

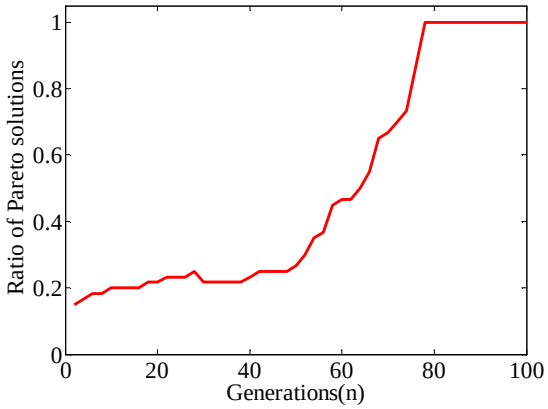

Figure 7 –Evolutionary process of Pareto solution

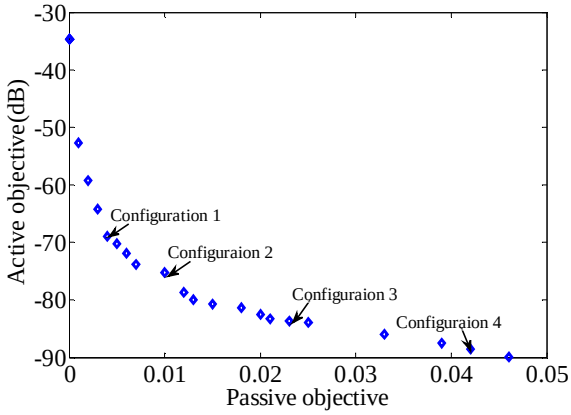

Figure 8 –The Pareto front

The ACLD configurations for the first vibration mode control is optimized using the above integrated optimization strategy. Figure 7 displays the evolutionary process of the Pareto solutions, and the solutions convergences well. Figure 8 shows the Pareto front, and the objectives distributes evenly in a curve. Four different configurations listed in table 2 are selected to analyze the effectiveness of the optimization method.

Table 2 –The pareto solutions and the first mode frequency

Configuration Number	Locations of PCLD patches	h_v/m	h_c/m	Locations of Actuators	First mode frequency/Hz
1	2,3,6,7,18,19,29,32	0.002	0.0011	2,3	14.868
2	2,3,6,714,15,17,20,	0.0015	0.0007	2,3	17.448
3	1,4,5,8,9,12,18,19	0.0017	0.0009	1,4	20.053
4	2,3,6,7,10,11,14,15	0.002	0.001	2,3	23.199

A comparison of frequency responses among different ACLD configurations and base plate is

illustrated in figure 9.It is very clear that the vibration of first mode can be surpressed obviously when the base late treated with the four ACLD configurations. And with passive objectives increasing, the better vibration surpression for first bending mode can be achieved.

A PD controller is designed to simulate the active vibraion control results when the four optimal locations of actuators are employed. In the simulation, the control voltages are set to be the same, 100V, and the ACLD/plates are vibrating with the same amplitude(displacement). Figure 10 shows the simulation results for different ACLD patches acting as actuators. It illustrates that with active objectives increasing, the vibraion of first bending mode can be surpressed much more.

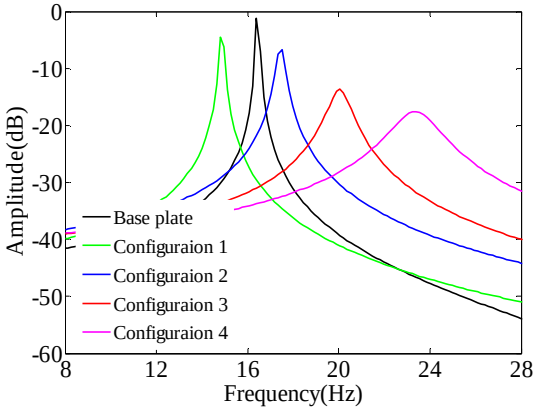

Figure 9 –Frequency responses for different ACLD configurations

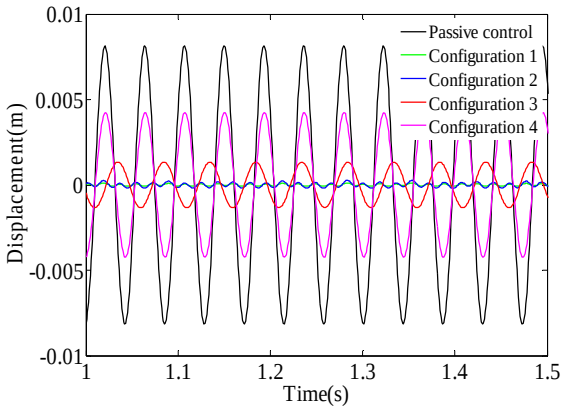

Figure 10 –Active control results for different Actuators

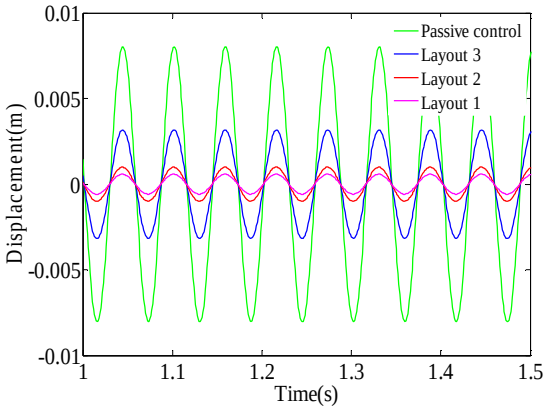

Figure 11 –Active control results for local optimal ACLD patches configurations

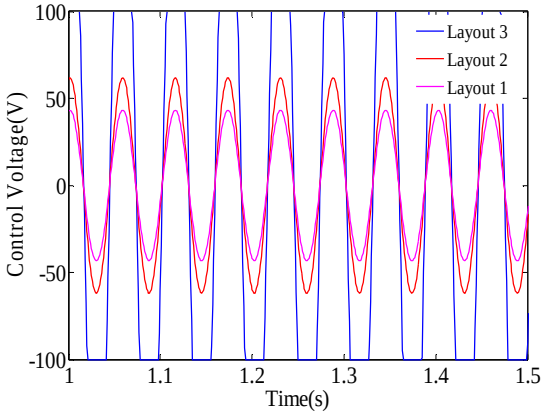

Figure 12 –Control voltage

The local optimal locations for ACLD patches acting as actuators are analyzed in any global optimal ACLD configurations. For simplicity, only configuration 2 is selected to investigate. The optimal location layout (2,3) is named as layout 1, and other two arbitrary layouts (6,7) and (15,17) are layout 2 and layout 3. A PD controller is designed to simulate the active results when the three ACLD layouts are employed. In the simulation, the parameters of the controller are the same, besides that of the disturbance. Figure 11 and 12 display the simulation results and the control voltage. It can be seen that the better vibration suppression can be obtained with smaller control voltage when layout 1 is used. Furthermore, it can be conclude that the ACLD patches acting as actuators should be located at the root of the cantilever structure.

Based on the above discussions, it can be seen that the integrated multi-objective optimization procedure is very effective to obtain the global ACLD configurations for ACLD/structure,and the local optimal actuators locations from ACLD configurations. The optimal results can supply variable ACLD configurations according to design requirements.

5. CONCLUSIONS

In this paper, the multi-objective optimization of ACLD/plate is developed based on the finite element method (FEM).A integrated strategy is proposed to optimize the performance of passive control and active control for ACLD/structure. Combining with direct search method, the improved

non-dominated genetic algorithm (INSGA-II) is developed to solve the optimization problem. The vibration control performance of the first bending mode of the ACLD/plate is optimized based on the method. The results show that it is very effective to obtain optimal vibration control results.

ACKNOWLEDGEMENTS

This work was supported by Nature Science Foundation of China (No.50775225,No.50875270), Chongqing Science and Technology Committee (No.CSTC2008 AC6097, No.CSTC2008BA6025). These financial supports are gratefully acknowledged.

REFERENCES

1. Ray M C., Baz A. Control of nonlinear vibration of beams using active constrained layer damping. Journal of Vibration and Control, Vol. 7, Issue 4, 2001, p. 539-549.
2. Kumar Navin., Singh S P. Vibration and damping characteristics of beams with active constrained layer treatments under parametric variations. Materials &Design, Vol.30, Issue 10, 2009, p. 4162-4172.
3. Ray M C., Shivakumar J. Active constrained layer damping of geometrically nonlinear transient vibrations of composite plate using piezoelectric fiber-reinforced composite. Thin-Walled Structures, Vol.47, Issue 2, 2009, p.178-189.
4. Ling Zheng, Dongdong Zhang and Yi Wang. Vibration and damping characteristics of cylindrical shells with active constrained layer damping treatments. Smart material and Structure, Vol. 20, Issue 2, 2011,p. 025008.
5. Ro J., Baz A. Optimum Placement and Control of Active Constrained Layer Damping using Mode Strain Energy Approach. Proceedings of the SPIE. Vol. 3329, 1998, p.844-855.
6. Kung S W., Singh R. Development of approximate methods for the analysis of patch damping design concept. Journal of Sound and Vibration, Vol. 219, Issue 5,1999, p.785-812.
7. Zheng H., Cai C and Pau G S H. A comparative study on optimization of constrained layer damping treatment for structural vibration control. Thin-Walled Structures, Vol. 44, Issue 8, 2006, 886-896.
8. Al-Ajmi M., Boursili R. Optimum design of segmented passive constrained layer damping treatment through genetic algorithms. Mechanics of Advanced Materials and Structures, Vol. 15, Issue 1, 2008, p. 250-257.
9. Zheng Ling., Xie Ronglu and Wang Yi. Optimal placement of constrained damping material in structures based on optimality criteria. Journal of Vibration and Shock, Vol. 11, 2010, p.156-159+179+259-260
10. Li Yinong., Xie Ronglu and Zheng Ling. Topology optimization for constrained layer damping material in structures using ESO method. Journal of Chongqing University, Vol. 8, 2010, p.1-6.
11. Nguyen, Quan., Tong Liyong, Gu Yuanxian. Evolutionary piezoelectric actuators design optimisation for static shape control of smart plates. Computer Methods in Applied Mechanics and Engineering, Vol.197, Issue 1-4, 2007,47-60.
12. Qiu, Zhi-cheng, Zhang Xian-min, Wu Hong-xin and Zhang Hong-hua. Optimal placement and active vibration control for piezoelectric smart flexible cantilever plate. Vol.301, Issue 3-5, 2007,521-543.
13. Bruant I., Gallimard L., Nikoukar S. Optimal piezoelectric actuator and sensor location for active vibration control, using genetic algorithm. Journal of Sound and Vibration, Vol.329, Issue 10, 2010, p.1615-1635.
14. Sohn J W., Choi S B and Kim, H S. Vibration control of smart hull structure with optimally placed piezoelectric composite actuators. International Journal of Mechanical Sciences, Vol.53, Issue 8, 2011,p.647-659.
15. Li W P., Huang H. Integrated optimization of actuator placement and vibration control for piezoelectric adaptive trusses. Journal of Sound and Vibration, Vol. 32 Issue 1, 2013,p.17-32.
16. Hau L C., Fung E H K. Multi-objective optimization of an active constrained layer damping treatment for shape control of flexible beams. Smart Material and Structure, Vol.13, Issue 4, 2005, p.896-906.
17 Araújo A L., Madeira J F.A., Mota Soares C M and Mota Soares C A. Optimal design for active damping in sandwich structures using the Direct MultiSearch method.Composite Structure, Vol.105, 2013,p.29-34.
18. Zhang Dongdong, Zheng Ling. Active Vibration Control of Plate Partly Treated with ACLD Using Hybrid Control. International Journal of Aerospace Engineering, Vol.2014, 2014, p.1-12.
19. McTavish D J., Hughes P C. Modeling of linear viscoelastic space structures. American Society of Mechanical Engineers, Journal of Vibration and Acoustics, Vol.115, 1993, p.103-110.

20. Deb Kalyanmoy. An efficient constraint handling method for genetic algorithms. Computer Methods in Applied Mechanics and Engineering, Vol. 186, Issue 2-4, 2000, p.311-338.
21. Deb Kalyanmoy. Multi-objective Optimization using Evolutionary Algorithms. JOHN WILEY& SONS Inc.New York, 2008.
22. Deep Kusum., Singh Krishna Pratap., Kansal M L and Mohan C. A real coded genetic algorithm or solving integer and mixed integer optimization problems. Applied Mathematics and Computation, Vol. 212, Issue 2,2009, p.505-518.